Tuning the Activity and Selectivity of Phenylacetylene Hydrosilylation with Triethylsilane in the Liquid Phase over Size Controlled Pt Nanoparticles

Dorina G. Dobó [1], Dániel Sipos [1], András Sápi [1,4],* , Gábor London [2], Koppány L. Juhász [1], Ákos Kukovecz [1] and Zoltán Kónya [1,3]

[1] Department of Applied and Environmental Chemistry, University of Szeged, H-6720 Szeged, Hungary; d.dorina@chem.u-szeged.hu (D.G.D.); sipos.herr.dani@gmail.com (D.S.); koppany.juhasz@chem.u-szeged.hu (K.L.J.); kakos@chem.u-szeged.hu (A.K.); konya@chem.u-szeged.hu (Z.K.)

[2] Institute of Organic Chemistry, Research Centre for Natural Sciences, Hungarian Academy of Sciences, Budapest, Magyar tudósok körútja 2, 1117 Budapest, Hungary; london.gabor@gmail.com

[3] MTA-SZTE Reaction Kinetics and Surface Chemistry Research Group, University of Szeged, H-6720 Szeged, Hungary

[4] Institute of Environmental and Technological Sciences, University of Szeged, H-6720 Szeged, Hungary

* Correspondence: sapia@chem.u-szeged.hu; Tel.: +36-30-325-0021

Abstract: Pt nanoparticles with controlled sizes between 1.6–7.0 nm were anchored onto the surface and pores of SBA-15 silica support. The catalysts were characterized by TEM-ED, BET, XRD, and ICP-MS techniques and were tested in liquid phase hydrosilylation of phenylacetylene with triethylsilane. The activity of the 7.0 nm Pt nanoparticles anchored onto the surface of SBA-15 in hydrosilylation (TOF = 0.107 molecules·site^{-1}·s^{-1}) was ~2 times higher compared to the 5.0 nm Pt/SBA-15 (TOF = 0.049 molecules·site^{-1}·s^{-1}) catalyst and ~10 times higher compared to the 1.6 nm Pt/SBA-15 (TOF = 0.017 molecules·site^{-1}·s^{-1}) catalyst. Regarding the selectivity, bigger nanoparticles produced more vinylsilane-type products (α- and β-(E)-products) and less side products (mainly ditriethylsilane, triethyl(1-phenylethyl)silane and triethyl(phenethyl)silane derived likely from the reduction of the vinylsilane products). However, the selectivity towards the β-(*E*)-triethyl(styryl)silane was higher in the case of 1.6 nm Pt/SBA-15 catalyst compared to 5.0 nm Pt/SBA-15 and 7.0 nm Pt/SBA-15, respectively, which can be attributed to the beneficial effect of the size differences of the Pt nanoparticles as well as the differences of the quality and quantity of Pt/SiO$_2$ interfaces.

Keywords: controlled size Pt nanoparticles; hydrosilylation; catalysis by design; Pt/SiO$_2$ interface

1. Introduction

Organosilicon compounds obtained by hydrosilylation of unsaturated C-C-bonds are of great interest both from industrial and academic point of view [1]. On one hand, they are the building blocks of several polymeric materials, while vinylsilanes derived from acetylenes are greener alternatives of organotin, organozinc, or organoboron compounds in transition metal catalyzed cross-coupling reactions [2]. The preparation of vinylsilanes from alkynes, however, could result in the formation of diverse product structures, thus controlling the selectivity of the reaction is of great importance. Transition metal catalysts have been employed in hydrosilylation reactions, among which heterogeneous ones are gaining importance within the frames of green chemistry [3–13]. Supported

Pt [3–5,7–9,14], Pd [13], Pd alloys [15,16], and Au [6,10,12] particles have been shown to be efficient heterogeneous hydrosilylation catalysts leading mostly to the β-(*E*) product with high selectivity (Figure 1).
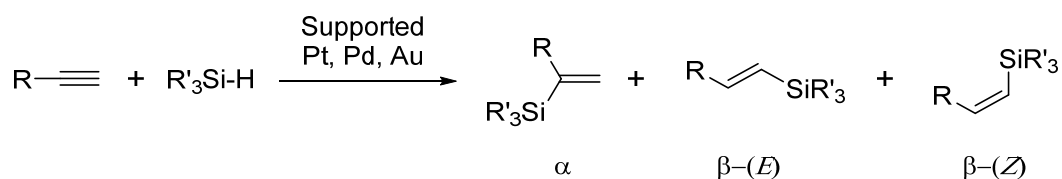
Figure 1. Transition metal catalyzed hydrosilylation of terminal acetylenes leading to isomeric vinlysilanes.

In contrast with extensive efforts targeting high selectivities, the effect of metal particle size on hydrosilylation of acetylenes has rarely been reported in the literature [6,17], although the effect of particle size and morphology could have a pronounced effect of the outcome of the reaction.

UHV as well as high pressure and in situ (e.g., sum frequency generation infrared spectroscopy) techniques proved that surface chemical processes are mostly structure sensitive reactions. The activation energy of the hydrogenation of benzene towards cyclohexane is approximately two times smaller on hexagonal Pt(111) surfaces compared to square Pt(100) surfaces [18]. Pt(100) and Pt(13,1,1) were four times more active in isobutene isomerization towards *n*-butane compared to Pt(111) and Pt(10,8,7) surfaces [19]. In the case of metal nanoparticles with the size of 1–10 nm, the concentration of the surfaces with different Miller indices are drastically changing as the size of the particles are changing. Beside the surface-to-volume ratio, the number of the steps and kinks, the surface rearrangement compared to bulk counterpart under reaction conditions and the concentration of the different Miller indices could result in activity and selectivity differences of metallic nanoparticles with different size.

Hence, the synthesis as well as the catalytic activity and selectivity of size controlled metallic nanoparticles have been extensively studied [20–25]. For instance, in the gas phase, Rh nanoparticles with smaller sizes showed higher activity in CO oxidation [26]. However, Pt nanoparticles with bigger size (8–11 nm) were more active in lightweight hydrocarbon oxidation compared to smaller (1–4 nm) nanoparticles [27].

In this study, we prepared Pt nanoparticles with controlled size between 1.6–7.0 nm and anchored them onto the surface and pores of SBA-15 silica support. We characterized the catalysts with TEM-ED, BET, XRD, and ICP-Ms techniques and tested them in liquid phase hydrosilylation reactions at 70 °C.

We found that the activity of the 7.0 nm Pt nanoparticles anchored onto the surface of SBA-15 was ~2 times and ~10 times faster compared to 5.0 nm Pt/SBA-15 and 1.6 nm Pt/SBA-15, respectively. In the case of selectivity, bigger nanoparticles produced more vinylsilane-type products (α- and β-(E)-products) and less side products (mainly ditriethylsilane, triethyl(1-phenylethyl)silane and triethyl(phenethyl)silane derived likely from the reduction of the vinylsilane products). However, the selectivity towards the β-(*E*)-triethyl(styryl)silane was found to be higher in the case of the 1.6 nm Pt/SBA-15 catalyst.

2. Results and Discussion

Pt nanoparticles were prepared in ethylene-glycol from different Pt-salt precursors (hexachloroplatinic acid, tetrachloro-platinate, and platinum(II) acetylacetonate) while PVP was used as capping agent and surface controlling agent. Controlled size Pt nanoparticles were observed by TEM with narrow size distribution with sizes of 1.6 ± 0.5 nm, 5.0 ± 1.0 nm, and 7.0 ± 1.0 nm (Figure 2).
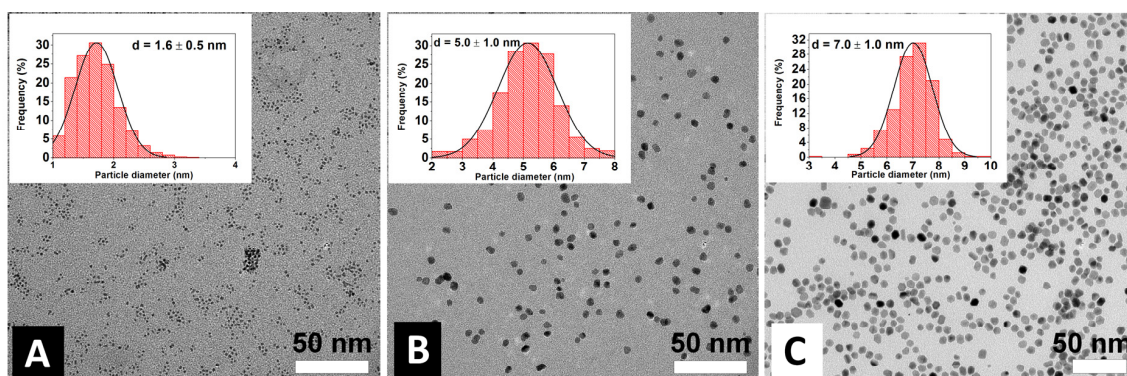
Figure 2. Typical TEM images of size controlled Pt nanoparticles with the sizes of (**A**) 1.6 ± 0.5 nm; (**B**) 5.0 ± 1.0 nm; and (**C**) 7.0 ± 1.0 nm.

SBA-15 silica was used as support material for the controlled size Pt nanoparticles in the hydrosilylation reactions. SBA-15 was successfully synthesized from TEOS precursor resulted in a mesoporous structure with pores of 2–4 nm in diameter (Figure 3). The amorphous nature of silica was identified by XRD as well as type V isotherm characteristic for mesoporous materials were observed by BET measurements (Figure 4). A typical SBA-15 sample has a specific surface area of 798 m^2/g with an average pore diameter of 2.3 nm correlates well with TEM images. Size-controlled Pt nanoparticles were anchored onto the surface and into the pores of the SBA-15 silica support by a sonication process resulting in different Pt/SBA-15 catalysts (Figure 3).

(**a**)　　　　　　　　　　(**b**)　　　　　　　　　　(**c**)
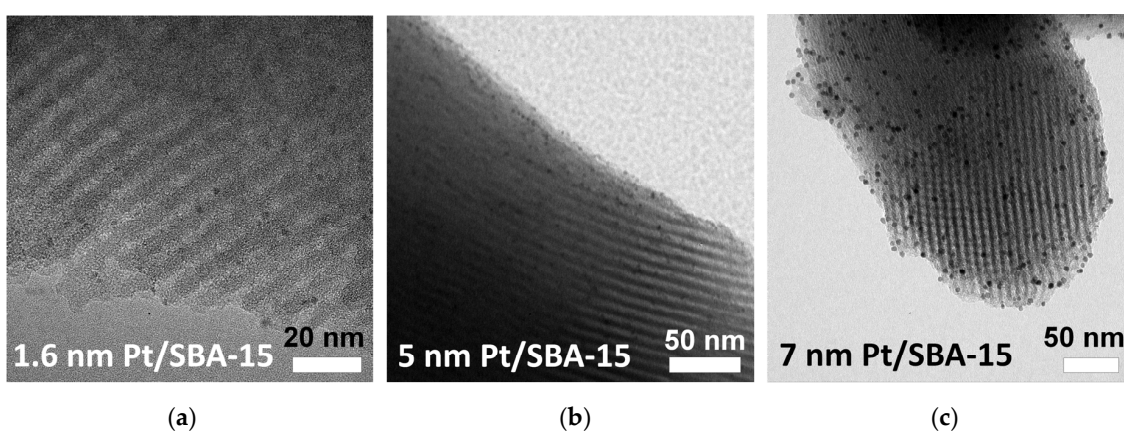
Figure 3. SBA-15 supported Pt nanoparticles with the size of (**a**) 1.6 nm; (**b**) 5.0 nm; and (**c**) 7.0 nm.
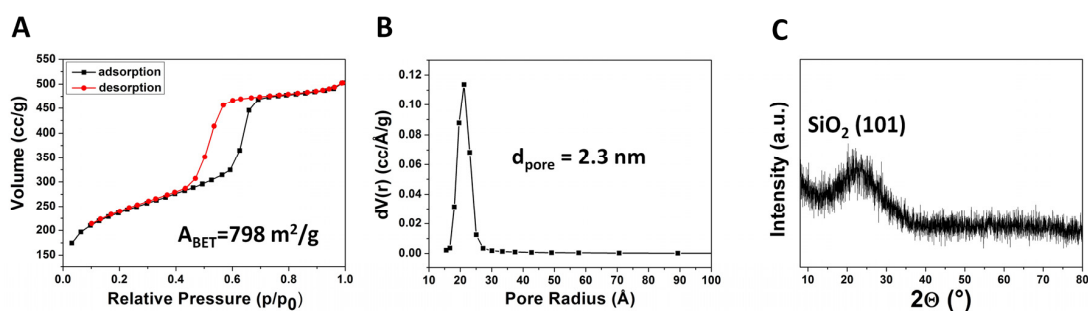
Figure 4. (**A**) BET isotherm and (**B**) corresponding pore diameter distribution as well as (**C**) powder XRD pattern of pure SBA-15 silica support.

The as-prepared Pt/SBA-15 catalysts were tested in liquid phase hydrosilylation of phenylacetylene with triethylsilane at 70 °C in THF. The main vinylsilane products of the reaction were triethyl(1-phenylvinyl)silane (α-product, **1**) and (*E*)-triethyl(styryl)silane (β-(*E*)-product, **2**) (Figure 5). It has to be noted, that the (*Z*)-triethyl(styryl)silane (β-(*Z*)-product, **3**) was not detected.
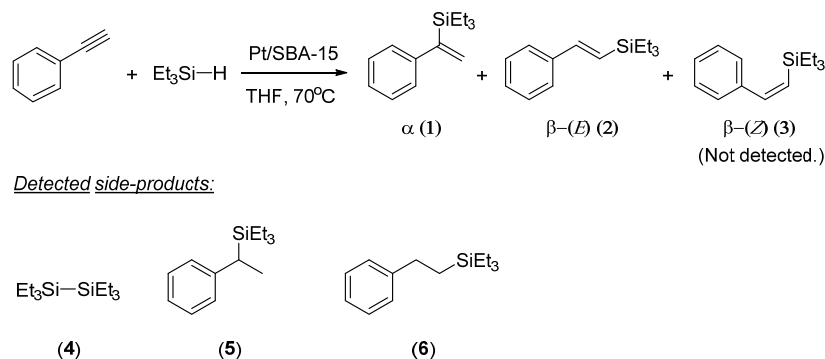
Figure 5. Hydrosilylation of phenylacetylene with triethylsilane leading to vinylsilanes **1** and **2** and the detected side products **4**–**6**.

Apart from vinylsilanes **1** and **2**, dimerized triethylsilane (**4**) and the saturated derivatives of vinylsilane **1** and **2**—namely, triethyl(1-phenylethyl)silane (**5**) and triethyl(phenethyl)silane (**6**)—were detected as side products. The latter two compounds likely formed via the hydrogenation of **1** and **2** with triethylsilane being the hydrogen source. The catalytic reactions were monitored by GC-MS technique, by which the above mentioned products were identified.

The conversions were 7.4, 3.8, and 6.8% for 1.6 nm Pt/SBA-15, 5.0 nm Pt/SBA-15, and 7.0 nm Pt/SBA-15 catalysts, respectively after 6 h of reactions. The activity of the 7.0 nm Pt nanoparticles anchored onto the surface of SBA-15 in hydrosilylation (TOF = 0.107 molecules·site^{-1}·s^{-1}) was ~2 times higher compared to the 5.0 nm Pt/SBA-15 (TOF = 0.049 molecules·site^{-1}·s^{-1}) catalyst and ~10 times higher compared to the 1.6 nm Pt/SBA-15 (TOF = 0.017 molecules·site^{-1}·s^{-1}) catalyst (Figure 6A).
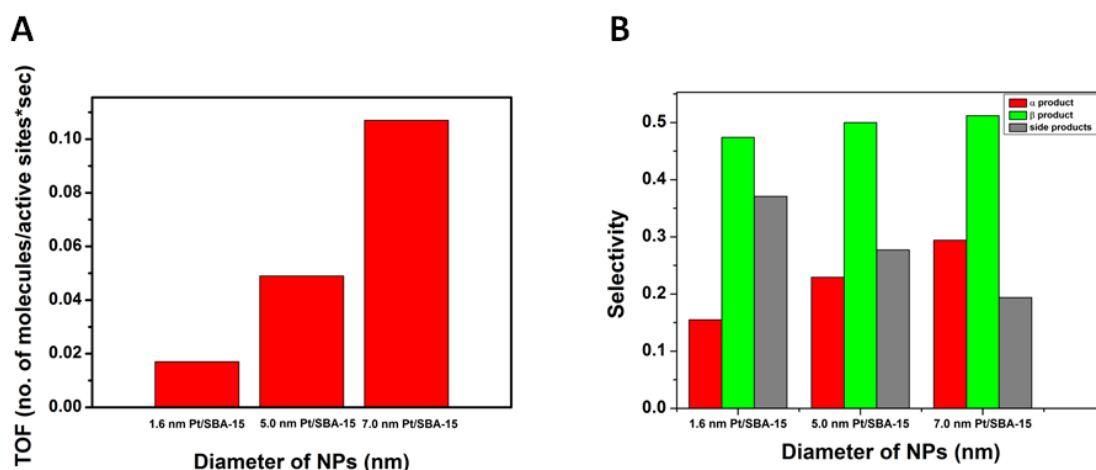
Figure 6. (**A**) Catalytic activity and (**B**) selectivity of hydrosilylation reactions over size controlled Pt nanoparticles in the liquid phase at 70 °C.

This difference in activity could be attributed to the size differences of the nanoparticles, which resulted in different surface-to-volume ratios, different concentrations of the different Miller indices facets on the surfaces, as well as the different surface rearrangements under reaction conditions. On the other hand, it is explored that the Pt-SiO$_2$ interface can play an important role in catalytic activity and

selectivity [28–30]. Due to the different sizes and positions of the Pt nanoparticles on the surface as well as in the pores of the SBA-15 support, Pt-SiO$_2$ interfaces with different quantities and qualities are formed.

Regarding selectivity, bigger nanoparticles produced more vinylsilane products **1** and **2** and less side products (**4**–**6**) (Figure 6B). In the case of 7.0 nm Pt/SBA-15 catalyst, selectivity towards the side products (19%) was ~1.5 and 2 times higher compared to 5.0 nm Pt/SBA-15 (27%) and 1.6 nm Pt/SBA-15 (37%) catalysts, respectively. Considering that both the hydrosilylation reaction leading to the desired vinylsilanes **1** and **2** and the triethylsilane mediated hydrogenation leading to alkanes **5** and **6** are occurring on the Pt-surface, the difference in activity could be due to additional confinement effects [31] in case of smaller Pt particles. When catalysts containing smaller Pt particles are used, that are largely inside the mesopores of the support, the vinlysilane products spend comparably more time in the proximity of the metal, giving higher probability of the subsequent reduction step. Overall, this leads to higher ratio of the side-products **5** and **6**. On the other hand, in cases of larger particles that are on the outer surface of the support, the product can leave the catalytic particle more easily following its formation, preventing further reactions leading to compounds **5** and **6**.

Regarding the selectivity between vinylsilanes **1** and **2**, all Pt nanoparticle based catalysts produced more β-(*E*) product (**2**) than α-product (**1**), however, their ratio was dependent on the size of the Pt particles. In the case of 1.6 nm Pt/SBA-15, the **2**/**1** ratio was 3, which value was decreased to 2.17 and 1.75 for 5.0 nm Pt/SBA-15 and 7.0 nm Pt/SBA-15, respectively, which can be attributed to the beneficial effect of the differences arisen from the size of the Pt nanoparticles as well as the Pt/SiO$_2$ interfaces.

In summary, bigger Pt particles are more active in hydrosilylation reactions of phenylacetylene with triethylsilane and they produce less side products. The smaller particles are less active, however their selectivity towards the β-(*E*) product (**2**) is higher. The results presented here show the importance of Pt particle size in the design of active and selective catalysts for hydrosilylation reactions. However, to further improve the selectivity between the required vinylsilane products the particle size and the pore-size as well as the nature of the support material have to be optimized parallel.

3. Materials and Methods

3.1. Synthesis of SBA-15 Mesoporous Silica

Synthesis of SBA-15 silica is well known [32]. Here, 8 g of pre-melted Pluronic-123 (Sigma-Aldrich, Budapest, Hungary) 60 mL distilled water and 240 mL of 2 M HCl (Molar Chemicals Ltd., Budapest, Hungary) solution were mixed at 40 °C for 2 h. After the P-123 was dissolved, 17 g of TEOS (Sigma-Aldrich, Budapest, Hungary) was added dropwise to the mixture at 40 °C and continuous stirring were applied for 20 h. Stirring was continued for 1.5 days at 60 °C. After the synthesis, the product was filtered and washed with distilled water. After washing, the product was heated to 100 °C with a heating rate of 2 °C·min^{-1} and aged for 5 h, then the temperature was elevated to 550 °C with a heating rate of 1 °C·min^{-1}. After 4 h of calcination, the product was collected.

3.2. Synthesis of 1.6 nm Platinum Nanoparticles

For 1.6 nm Pt nanoparticles, 29 mg of PtCl$_4$ (Sigma-Aldrich, Budapest, Hungary) and 50 mg of NaOH (Molar Chemicals Ltd., Budapest, Hungary) was dissolved in two separate portions of 2.5 mL of ethylene-glycol [33]. The solutions were then mixed and heated to 160 °C and kept at that temperature for 3 h under Ar atmosphere. After cooling down, 2.5 mL 1 M HCl (Molar Chemicals Ltd., Budapest, Hungary) solution was added to the black suspension and the nanoparticles were collected by centrifugation. The as-obtained nanoparticles were redispersed in 10 mL of 2.1 mg/mL PVP (Mw = 40.000) (Sigma-Aldrich, Budapest, Hungary) in ethanol with ultrasonication. The nanoparticles were washed with hexane precipitation/ethanol redispersion cycles. Finally, the product was dispersed in 10 mL ethanol.

3.3. Synthesis of 5.0 nm Platinum Nanoparticles

For 5.0 nm Pt nanoparticles, 0.04 g $Pt(C_5H_7O_2)_2$ and 35 mg polyvinylpyrrolidone (PVP, MW = 40,000, Sigma-Aldrich, Budapest, Hungary) were dissolved in 5 mL ethylene-glycol, and ultrasonicated for 30 min to get a homogenous solution [33]. The reactor was a three-necked round bottom flask, which was evacuated and purged with atmospheric pressure argon gas for several cycles to get rid of additional oxygen and water. After three purging cycles, the flask was immersed in an oil bath heated to 200 °C under vigorous stirring of the reaction mixture as well as the oil bath. After 10 min of reaction, the flask was cooled down to room temperature. The suspension was precipitated by adding acetone and centrifuging. The nanoparticles were washed by centrifuging with hexane and redispersed in ethanol for at least 2–3 cycles, and finally redispersed in ethanol.

3.4. Synthesis of 7.0 nm Platinum Nanoparticles

For 7.0 nm Pt nanoparticles, 40 mg H_2PtCl_4 (Sigma-Aldrich, Budapest, Hungary) and 40 mg polyvinylpyrrolidone (PVP, MW = 40,000, Sigma-Aldrich, Budapest, Hungary) were dissolved in 2.5 mL ethylene-glycol and mixed with a solution of 2.5 mL of 0.075 M NaOH (Molar Chemicals Ltd., Budapest, Hungary) in ethylene-glycol using a three-necked round bottom flask [33]. After 30 min of sonication, the flask was purged with atmospheric pressure argon gas. After three purging cycles, the flask was immersed into an oil bath heated to 160 °C under vigorous stirring of the reaction mixture as well as the oil bath. After 180 min of reaction, the flask was cooled down to room temperature. The pH of the suspension was neutralized with 2 M aqueous solution of HCl (Molar Chemicals Ltd., Budapest, Hungary). The suspension was precipitated by adding acetone. After precipitation, the particles were washed by centrifugation with hexane and redispersed in ethanol for at least 2–3 cycles, and finally stored in ethanol.

3.5. Preparation of the Silica Supported Pt Nanoparticle Catalysts

The different size of Pt nanoparticles and silica supports (SBA-15) were mixed together in ethanol and sonicated in an ultrasonic bath (40 kHz, 80 W) for 3 h to reach a nominal 1% of Pt loading [29,34]. The supported nanoparticles were collected by centrifugation. The products were washed with ethanol three times before they were dried at 80 °C overnight. For the ethanol decomposition reactions, the catalysts were pretreated as described later. The size of the Pt nanoparticles was determined by using TEM images. The number of the Pt nanoparticles loaded into the test samples were calculated by the results of TEM and inductively coupled plasma mass spectrometry (ICP-MS). The real concentrations of the 1.6 nm Pt/SBA-15, 5.0 nm Pt/SBA-15 and the 7.0 nm Pt/SBA-15 samples were 0.35, 0.81, and 0.33%, respectively. The calculation of the number of the active sites was based on these results assuming Pt nanoparticles with spherical shape and Pt (111) surfaces and that of every surface Pt atom is active in the reaction.

3.6. Characterization of the Catalysts

Imaging of the different silica supports, Pt nanoparticles and derived catalysts, as well as the size distribution of the nanoparticles was performed by an FEI TECNAI G2 20 X-Twin high-resolution transmission electron microscope (FEI, OR, USA) (equipped with electron diffraction) operating at an accelerating voltage of 200 kV. The samples were drop-cast onto carbon film coated copper grids from ethanol suspension.

XRD studies of the silica supports were performed on a Rigaku MiniFlex II instrument (Rigaku, Tokyo, Japan) with a Ni-filtered CuK_α source in the range of 2θ = 10–80°.

The specific surface area (BET method), the pore size distribution were determined by the BJH method using a Quantachrome NOVA 2200 gas sorption analyzer (Quantachrome, FL, USA) by N_2 gas adsorption/desorption at −196 °C. Before the measurements, the samples were pre-treated in vacuum (<~0.1 mbar) at 473 K for 2 h.

The loading of the Pt on the supported catalysts was determined by ICP-MS technique. The measurements were performed using an Agilent 7700x type ICP-MS spectrometer (Santa Clara, CA, USA). The sample uptake rate was 200 μL·min^{-1}. The ICP plasma and interface parameters were set according to the standard hot plasma configuration (e.g., RF forward power: 1550 W, argon carrier gas flow rate: 1.05 L/min, sampling depth: 8.0 mm). Fine tuning was performed before the analytical measurements using tuning solutions supplied by the manufacturer (G1820-60410, 5185–5959 Agilent Technologies, Santa Clara, CA, USA). All measurements were carried out using the He mode of the ORS^3 collision cell by monitoring the signal of ^{195}Pt isotope.

^{1}H NMR spectroscopy (Bruker AVANCE DRX 400, Billerica, MA, USA) was used to characterize vinylsilane products **1**–**3** (Figure 7).

3.7. Catalytic Hydrosilylation Reactions

Hydrosilylation of phenylacetylene with triethylsilane was used as a model reaction for exploring the heterogeneous catalytic hydrosilylation reaction over size-controlled Pt nanoparticles. In a typical reaction, phenylacetylene (55 μL, 0.5 mmol) and triethylsilane (80 μL, 0.5 mmol) were dissolved in THF (1 mL) followed by the addition of the catalyst (total of 25 mg; ~0.25 mg of metallic Pt). The mixture was heated at 70 °C for 6 h, centrifuged, and the supernatant was analyzed with GC-MS technique. The TOF values were calculated at the kinetic regime where the conversion was between 1–10%.

The main vinylsilane products triethyl(1-phenylvinyl)silane (α-product, **1**), (*E*)-triethyl(styryl)silane (β-(*E*)-product, **2**) and (*Z*)-triethyl(styryl)silane (β-(*Z*)-product, **3**) were prepared by using Pt/Al$_2$O$_3$ (E4759) catalyst under the same conditions described above, and analyzed by ^{1}H-NMR spectroscopy (Figure 2). The products isolated from the control reaction were used to assign the α-product (**1**) and the β-(*E*)-product (**2**) in subsequent GC-MS analyses.
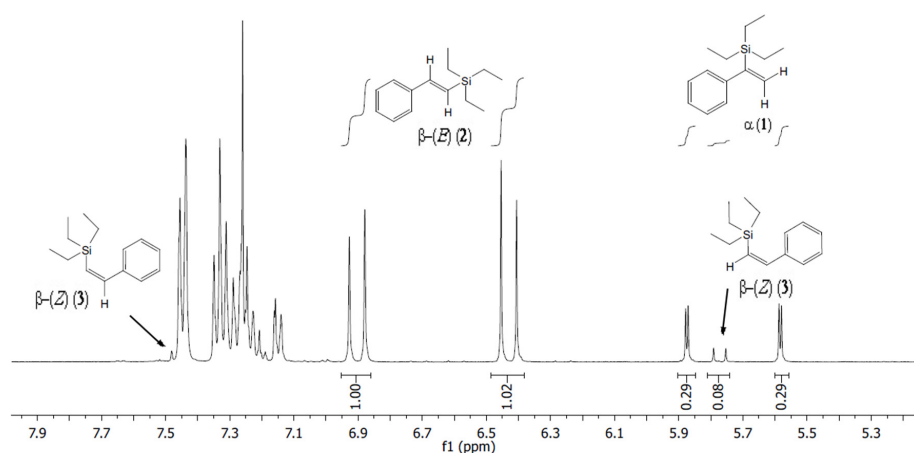
Figure 7. Characteristic ^{1}H NMR shifts of a mixture of vinyl-silane products **1**–**3** prepared using commercial Pt/Al$_2$O$_3$ (E4759).

4. Conclusions

Size controlled Pt nanoparticles showed size-dependent activity and selectivity in the case of phenylacetylene hydrosilylation with triethylsilane in the liquid phase. 7.0 nm Pt nanopartciles supported on the surface of SBA-15 silica has the highest activity compared to smaller Pt nanoparticles (1.6 nm and 5.0 nm). In the case of selectivity, smaller particles produced more β-(*E*) product (**2**) compared to α-product (**1**).

The results show that controlled size synthesis of Pt nanoparticles is a viable tool for tuning catalytic activity and selectivity in hydrosilylation reactions. Beside the particle size, the tuning of the pore size of the support—even if the support is inert—has to be considered in order to optimize well defined Pt/SiO$_2$ interfaces to design catalysts towards 100% activity and selectivity.

Author Contributions: S.A. and G.L. wrote the paper, designed the experiments and evaluate the data, J.K.L., D.S. and D.G.D. performed the experiments and evaluate the data, Á.K. and Z.K. contributed reagents, materials and instruments.

Conflicts of Interest: The authors declare no conflict of interest.

References

1. Ojima, I.; Li, Z.; Zhu, J. *The Chemistry of Organic Silicon Compounds*; ZVi, R., Apeloig, Y., Eds.; Wiley: Hoboken, NJ, USA, 1998.

2. Denmark, S.; Ober, M.H. Organosilicon Reagents: Synthesis and Application to Palladium-Catalyzed Cross-Coupling Reactions. *Aldrichimica Acta* **2003**, *3*, 75–85. [CrossRef]

3. Pagliaro, M.; Ciriminna, R.; Pandarus, V.; Béland, F. Platinum-Based Heterogeneously Catalyzed Hydrosilylation. *Eur. J. Org. Chem.* **2013**, *2013*, 6227–6235.

4. Alonso, F.; Buitrago, R.; Moglie, Y.; Ruiz-Martínez, J.; Sepúlveda-Escribano, A.; Yus, M. Hydrosilylation of alkynes catalysed by platinum on titania. *J. Organomet. Chem.* **2011**, *696*, 368–372. [CrossRef]

5. Alonso, F.; Buitrago, R.; Moglie, Y.; Sepúlveda-Escribano, A.; Yus, M. Selective hydrosilylation of 1,3-diynes catalyzed by titania-supported platinum. *Organometallics* **2012**, *31*, 2336–2342. [CrossRef]

6. Aronica, L.A.; Schiavi, E.; Evangelisti, C.; Caporusso, A.M.; Salvadori, P.; Vitulli, G.; Bertinetti, L.; Martra, G. Solvated gold atoms in the preparation of efficient supported catalysts: Correlation between morphological features and catalytic activity in the hydrosilylation of 1-hexyne. *J. Catal.* **2009**, *266*, 250–257. [CrossRef]

7. Cano, R.; Yus, M.; Ramón, D.J. Impregnated Platinum on Magnetite as an Efficient, Fast, and Recyclable Catalyst for the Hydrosilylation of Alkynes. *ACS Catal.* **2012**, *2*, 1070–1078. [CrossRef]

8. Hamze, A.; Provot, O.; Brion, J.D.; Alami, M. Regiochemical aspects of the platinum oxide catalyzed hydrosilylation of alkynes. *Synthesis (Stuttg)* **2007**, *13*, 2025–2036. [CrossRef]

9. Hu, W.; Xie, H.; Yue, H.; Prinsen, P.; Luque, R. Super-microporous silica-supported platinum catalyst for highly regioselective hydrosilylation. *Catal. Commun.* **2017**, *97*, 51–55. [CrossRef]

10. Ishikawa, Y.; Yamamoto, Y.; Asao, N. Selective hydrosilylation of alkynes with a nanoporous gold catalyst. *Catal. Sci. Technol.* **2013**, *3*, 2902. [CrossRef]

11. Jiménez, R.; Martínez-Rosales, J.M.; Cervantes, J. The activity of Pt/SiO_2 catalysts obtained by the sol-gel method in the hydrosilylation of 1-alkynes. *Can. J. Chem.* **2003**, *81*, 1370–1375. [CrossRef]

12. Psyllaki, A.; Lykakis, I.N.; Stratakis, M. Reaction of hydrosilanes with alkynes catalyzed by gold nanoparticles supported on TiO_2. *Tetrahedron* **2012**, *68*, 8724–8731. [CrossRef]

13. Reddy, C.B.; Shil, A.K.; Guha, N.R.; Sharma, D.; Das, P. Solid Supported Palladium(0) Nanoparticles: An Efficient Heterogeneous Catalyst for Regioselective Hydrosilylation of Alkynes and Suzuki Coupling of β-Arylvinyl Iodides. *Catal. Lett.* **2014**, *144*, 1530–1536. [CrossRef]

14. Chauhan, B.P.S.; Sarkar, A. Functionalized vinylsilanes via highly efficient and recyclable Pt-nanoparticle catalysed hydrosilylation of alkynes. *Dalton Trans.* **2017**, *46*, 8709–8715. [CrossRef] [PubMed]

15. Zhang, J.; Lu, G.; Cai, C.; Zhang, T.; Mou, C.-Y.; Su, D.-S.; Li, J.; Zhao, J.; Thieuleux, C.; Petit, M. Regio-and stereoselective hydrosilylation of alkynes catalyzed by SiO_2 supported Pd-Cu bimetallic nanoparticles. *Green Chem.* **2017**, *19*, 2535–2540. [CrossRef]

16. Miura, H.; Endo, K.; Ogawa, R.; Shishido, T. Supported Palladium–Gold Alloy Catalysts for Efficient and Selective Hydrosilylation under Mild Conditions with Isolated Single Palladium Atoms in Alloy Nanoparticles as the Main Active Site. *ACS Catal.* **2017**, *7*, 1543–1553. [CrossRef]

17. Rivero-Crespo, M.A.; Leyva-Pérez, A.; Corma, A. A Ligand-Free Pt_3 Cluster Catalyzes the Markovnikov Hydrosilylation of Alkynes with up to 10^6 Turnover Frequencies. *Chem. Eur. J.* **2017**, *23*, 1702–1708. [CrossRef] [PubMed]

18. Bratlie, K.M.; Kliewer, C.J.; Somorjai, G.A. Structure effects of benzene hydrogenation studied with sum frequency generation vibrational spectroscopy and kinetics on Pt(111) and Pt(100) single-crystal surfaces. *J. Phys. Chem. B* **2006**, *110*, 17925–17930. [CrossRef] [PubMed]

19. Somorjai, G.A.; Davis, S.M. Surface Science Studies of Catalysed Reactions on Platinum Surfaces. *Platin. Met. Rev.* **1983**, *27*, 54–65.

20. Park, J.; An, K.; Hwang, Y.; Park, J.-G.; Noh, H.-J.; Kim, J.-Y.; Park, J.-H.; Hwang, N.-M.; Hyeon, T. Ultra-large-scale syntheses of monodisperse nanocrystals. *Nat. Mater.* **2004**, *3*, 891–895. [CrossRef] [PubMed]

21. Xia, Y.; Xiong, Y.; Lim, B.; Skrabalak, S.E. Shape-controlled synthesis of metal nanocrystals: Simple chemistry meets complex physics? *Angew. Chem.* **2009**, *48*, 60–103. [CrossRef] [PubMed]

22. Tatsumi, H.; Liu, F.; Han, H.-L.; Carl, L.M.; Sapi, A.; Somorjai, G.A. Alcohol Oxidation at Platinum–Gas and Platinum–Liquid Interfaces: The Effect of Platinum Nanoparticle Size, Water Coadsorption, and Alcohol Concentration. *J. Phys. Chem. C* **2017**, *121*, 7365–7371. [CrossRef]

23. Sapi, A.; Liu, F.; Cai, X.; Thompson, C.M.; Wang, H.; An, K.; Krier, J.M.; Somorjai, G.A. Comparing the Catalytic Oxidation of Ethanol at the Solid–Gas and Solid–Liquid Interfaces over Size-Controlled Pt Nanoparticles: Striking Differences in Kinetics and Mechanism. *Nano Lett.* **2014**, *14*, 6727–6730. [CrossRef] [PubMed]

24. Alayoglu, S.; Krier, J.M.; Michalak, W.D.; Zhu, Z.; Gross, E.; Somorjai, G.A. In situ surface and reaction probe studies with model nanoparticle catalysts. *ACS Catal.* **2012**, *2*, 2250–2258. [CrossRef]

25. Alayoglu, S.; Aliaga, C.; Sprung, C.; Somorjai, G.A. Size and shape dependence on Pt nanoparticles for the methylcyclopentane/hydrogen ring opening/ring enlargement reaction. *Catal. Lett.* **2011**, *141*, 914–924. [CrossRef]

26. Grass, M.E.; Joo, S.H.; Zhang, Y.; Somorjai, G.A. Colloidally synthesized monodisperse Rh nanoparticles supported on SBA-15 for size-and pretreatment-dependent studies of CO oxidation. *J. Phys. Chem. C* **2009**, *113*, 8616–8623. [CrossRef]

27. Gololobov, A.M.; Bekk, I.E.; Bragina, G.O.; Zaikovskii, V.I.; Ayupov, A.B.; Telegina, N.S.; Bukhtiyarov, V.I. Platinum nanoparticle size effect on specific catalytic activity in *n*-alkane deep oxidation: Dependence on the chain length of the paraffin. *Kinet. Catal.* **2009**, *50*, 864–870. [CrossRef]

28. Yamada, Y.; Tsung, C.K.; Huang, W.; Huo, Z.; Habas, S.E.; Soejima, T.; Aliaga, C.E.; Somorjai, G.A.; Yang, P. Nanocrystal bilayer for tandem catalysis. *Nat. Chem.* **2011**, *3*, 372–376. [CrossRef] [PubMed]

29. Sápi, A.; Dobó, D.G.; Sebok, D.; Halasi, G.; Juhász, K.L.; Szamosvölgyi, A.; Pusztai, P.; Varga, E.; Kálomista, I.; Galbács, G.; et al. Silica-Based Catalyst Supports Are Inert, Are They Not? Striking Differences in Ethanol Decomposition Reaction Originated from Meso-and Surface-Fine-Structure Evidenced by Small-Angle X-ray Scattering. *J. Phys. Chem. C* **2017**, *121*, 5130–5136. [CrossRef]

30. Ewing, C.S.; Veser, G.; McCarthy, J.J.; Johnson, J.K.; Lambrecht, D.S. Effect of Support Preparation and Nanoparticle Size on Catalyst–Support Interactions between Pt and Amorphous Silica. *J. Phys. Chem. C* **2015**, *119*, 19934–19940. [CrossRef]

31. Solomonsz, W.A.; Rance, G.A.; Harris, B.J.; Khlobystov, A.N. Competitive hydrosilylation in carbon nanoreactors: Probing the effect of nanoscale confinement on selectivity. *Nanoscale* **2013**, *5*, 12200–12205. [CrossRef] [PubMed]

32. Zhao, D.; Huo, Q.; Feng, J.; Chmelka, B.F.; Stucky, G.D. Nonionic triblock and star diblock copolymer and oligomeric surfactant syntheses of highly ordered, hydrothermally stable, mesoporous silica structures. *J. Am. Chem. Soc.* **1998**, *120*, 6024–6036. [CrossRef]

33. Sápi, A.; Varga, A.; Samu, G.F.; Dobó, D.G.; Juhász, K.L.; Takacs, B.; Varga, E.; Kukovecz, A.; Kónya, Z.; Janáky, C. Photoelectrochemistry by Design: Tailoring the Nanoscale Structure of Pt/NiO Composites Leads to Enhanced Photoelectrochemical Hydrogen Evolution Performance. *J. Phys. Chem. C* **2017**, *121*, 12148–12158. [CrossRef] [PubMed]

34. Rioux, R.M.; Song, H.; Hoefelmeyer, J.D.; Yang, P.; Somorjai, G.A. High-surface-area catalyst design: Synthesis, characterization, and reaction studies of platinum nanoparticles in mesoporous SBA-15 silica. *J. Phys. Chem. B* **2005**, *109*, 2192–2202. [CrossRef] [PubMed]